*Desalination and Water Treatment*
www.deswater.com

doi: 10.5004/dwt.2022.28730

269 (2022) 262–268
September

# Effect of a magnetic field on water crystallization in tunnel drainage pipes in karst areas

Fabo Liu[a], Min Xu[b], Shiyang Liu[c,d,*], Huaming Li[a], Yongqi Geng[c,d]

[a]*Sichuan Lehan Expressway Co., Ltd., Leshan 614200, China*
[b]*Leshan Traffic Engineering Construction Co., Ltd, Sichuan 614000, China*
[c]*State Key Laboratory of Mountain Bridge and Tunnel Engineering, Chongqing 400074, China, email: cqjtulsy@163.com (S. Liu)*
[d]*College of Civil Engineering, Chongqing Jiaotong University, Chongqing 400074, China*

Received 3 June 2021; Accepted 18 July 2022

**ABSTRACT**

In order to study the inhibitory effect and mechanism of magnetic fields on the crystallization of tunnel drainage pipes in karst areas, a 20-d experiment was performed in magnetic fields of six different intensities in the laboratory, with polyvinyl chloride (PVC) coiled pipes simulating drainage pipes in a magnetic field environment and a solution of calcium chloride and sodium bicarbonate simulating groundwater in Karst areas. The Leshan-Hanyuan Express Way project is the background of the experiment. The crystallization rules in this experiment are determined by the experimental crystal quality and X-ray diffraction patterns. A calcite crystal simulation model was built to calculate the changes in the magnetic field. It was found that the magnetic field reduced the quantity of crystals. As the magnetic flux density increases, the number of crystals decreases to the critical magnetic flux density of 0.1 T, and then remains constant as the magnetic flux density increases further. In some cases, the magnetic field can change the form of calcium carbonate ($CaCO_3$) from a stable crystal to an unstable one. When the magnetic flux density is increased beyond the critical value of 0.5 T, the crystal form hardly changes. Temperature has no significant effect on the number of crystals formed in the drain under a magnetic field. The test results have important guiding significance for the development of technology for preventing and controlling crystal blockage of tunnel drainage pipes.

*Keywords:* Magnetic field; Tunnel in karst area; Crystallization in drainage pipe; Magnetic flux density; Temperature

## 1. Introduction

With the acceleration of China's modernization, the construction of railways and expressways has developed by leaps and bound. There are many tunnels in the karst area of southwest China. The water in this region is nearly saturated with $HCO_3^-$ and high in $Ca^{2+}$. As groundwater flows into the drainage pipes, calcium carbonate ($CaCO_3$) crystals calcium carbonate crystals will slowly form upon the interior wall of the tunnel and eventually block the drainage system (Fig. 1). This seemingly trivial drainage pipe blockage represents a potential safety risk for the lining structure of the entire tunnel and the effective and smooth operation of the drainage system.

Hasson et al. [1] proposed a scaling rates model for the $CaCO_3$ deposition. Zhu [2] showed that the conditional solubility product of $CaCO_3$ depends on the solution pH. Liu [3] used the DBL model to forecast the deposition rate of calcite in a particular area. The factors leading to crystallization and scaling in pipes include high contents of water, bacteria, hyper salinity and dissolved $H_2S$, $CO_2$, $O_2$ or other corrosive gases in the medium [4]. A magnetic field mainly affects

* Corresponding author.

the growth rate and form of $CaCO_3$ crystal by changing the structure of water clusters [5].

The form of $CaCO_3$ crystals formed in lignin solution is different from that in pure water. The $CaCO_3$ crystals formed in a lignin solution have a calcite structure with dumbbell, spherical, elliptical and rugby-ball-like shapes. Both the lignin concentration and temperature of the growth system have a significant impact on the form and appearance of $CaCO_3$ crystals. During the crystallization of $CaCO_3$, there is interaction between $CaCO_3$ and lignin [6]. The magnetic treatment inhibits the crystal formation, with an induction period of about 8 min, and the crystallization rate decreases by 75.3% compared with the solution without magnetic treatment. A magnetic field affects $CaCO_3$ crystallization through scale-forming anions. The magnetic memory effect lasts for at least 72 h [7]. Based on the crystal growth kinetics, Larsen et al. [8] studied the scaling mechanism of $CaCO_3$ in an indoor core flooding test. Taheri et al. [9] studied the damage to reservoir caused by carbonate scaling during waterflooding in Iranian oil fields via an indoor simulation experiment. Charpentier et al. [10] have studied the scaling of $CaCO_3$ and barium sulfate in sub-surface equipment through dynamic experiments. High voltage electric field can hinder calcium ions from combining with carbanions to a certain extent, at the same time, it can reduce the bonding of calcium ions and carbanions on the calcite growth face also promote the dissolution of scale [11]. As the temperature rises, the scale amount of the system increases [12]. $SO_4^{2-}$ has less impact on calcite than $PO_4^{3-}$ [13]. The addition of $SO_4^{2-}$ slows down the crystallization process [14]. Deposits first within the rough structures on a pipe surface. If the quantity of deposits is sufficient to fill in the rough structures to form a smooth surface, a similar scaling curve to that of a smooth pipe is observed [15]. $PO_4^{3-}$ can significantly reduce the formation of calcite under constant and supersaturated conditions (temperature: 25°C, pH: 9.0 and 10.0) [16]. With the continuous increase of magnesium ion concentration, the deposition form of $CaCO_3$ gradually changed from calcite to aragonite [17]. Calcite crystals form at room temperature (25°C). Increasing the solution temperature above room temperature results in aragonite formation [18]. Increasing the Cr(VI) concentration will lead to the inhibition of calcite nucleation and growth and promote the generation of metastable polymorphic substances, such as aragonite and vaterite [19]. The quantity of scale in a system is not significantly affected by $HCO_3^-$ and can be reduced by increasing the initial $Cl^-$ concentration [20].

Experts and scholars worldwide have expressed concern regarding the blockage of a drainage system by crystals. The aforementioned study results cannot be directly applied to guide effective prevention of this problem. In this study, we performed an indoor experiment in which electric coils were wound around polyvinyl chloride (PVC) pipes to induce a magnetic field, which would separate cations and anions from flowing water and inhibit crystallization and prevent pipe blockage [21–24]. The influence of magnetic field intensity on the crystallization in tunnel drainage pipes in karst area was studied and the experimental crystals were analyzed by X-ray diffraction (XRD). Calcite crystal simulation model was established and the transformation rule of calcite crystal under magnetic field was studied.

Fig. 1. Drainage pipe blocked by crystals in the Baoligang Tunnel along the Emei-Hanyuan Expressway.

## 2. Crystals in groundwater from a tunnel in a karst area

Zou et al. [25] tested and analyzed the groundwater in tunnels in karst areas. Most of the water was found to contain carbonate, which is corrosive and can damage the tunnel lining structure and affect the drainage system over a long period of time. The contents of calcium, magnesium, sulfate and bicarbonate in groundwater of Baoligang tunnel on Emei Hanyuan expressway are relatively high. Considering the principle of strong acid replacing weak acid and the principle of reversible reaction, Eqs. (1)–(10) show the chemical reactions in a drainage pipe. We used these equations in conjunction with the results of a water quality analysis to deduce that $CaCO_3$ is the main component of the scale blocking the drainage system in the Baoligang Tunnel.

$$Ca^{2+} + CO_3^{2-} \rightarrow CaCO_3 \quad (1)$$

$$Mg^{2+} + CO_3^{2-} \rightarrow MgCO_3 \quad (2)$$

$$MgCO_3 + Ca^{2+} \rightarrow CaCO_3 + Mg^{2+} \quad (3)$$

$$Ca^{2+} + SO_4^{2-} \rightarrow CaSO_4 \quad (4)$$

$$CaSO_4 + CO_3^{2-} \rightarrow CaCO_3 + SO_4^{2-} \quad (5)$$

$$Ca^{2+} + HCO_3^- \leftrightarrow CaCO_3 + H^+ \quad (6)$$

$$Ca^{2+} + 2HCO_3^- \leftrightarrow CaCO_3 + CO_2 + H_2O \quad (7)$$

$$Mg^{2+} + 2HCO_3^- \leftrightarrow MgCO_3 + CO_2 + H_2O \quad (8)$$

$$Ca^{2+} + CO_2 + H_2O \leftrightarrow CaCO_3 + 2H^+ \quad (9)$$

$$Ca^{2+} + HCO_3^- + OH^- \rightarrow CaCO_3 + H_2O \quad (10)$$

## 3. Effect of a magnetic field on crystallization in a tunnel drainage pipe in a karst area

### *3.1. Effect of the magnetic flux density on crystallization in a tunnel drainage pipe*

#### *3.1.1. Indoor test*

$CaCl_2$ (AR) and $NaHCO_3$ (AR) solutions are used to simulate groundwater in karst area. We wound 253, 424, 697, 962, 1,482 and 1,989 turns of coils around a 32-mm-diameter PVC pipe and created an induction field by energizing the coils. For each coil setting, five 20-cm-long PVC pipes were used as the test group, and a PVC pipe without coils was used as the control. A transformer and power source were turned on to produce a magnetic field in each PVC pipe. The magnetic flux densities of the six coils were 0.02, 0.05, 0.08, 0.1, 0.5, and 1 T respectively. In order to simulate the actual flow velocity in the drainage pipe of Baoligang tunnel, the flow speed in the drainage pipe is maintained at 35 cm/s by using a velocimeter. The indoor temperature was controlled at approximately 291 K. The test cycle was 20 d. Saturated solutions of $CaCl_2$ and $NaHCO_3$ were used in the test. Each test pipe was dried and weighed at the end of the test. The results were compared and analyzed. The test procedure is shown in Fig. 2.

Fig. 2. Indoor test procedure.

#### *3.1.2. Test results*

##### *3.1.2.1. Effect of the magnetic field on the quantity of calcium carbonate crystals in a tunnel drainage pipe*

The pipes wound with coils producing magnetic fields with different intensities were dried and weighed at the end of the test to calculate the difference in the crystal quantity between each test group and the control before determining the average crystal quantity produced under each magnetic field. The result is shown in Fig. 3. Under all other conditions unchanged, the crystal quantity decreases as the magnetic flux density increases. When the magnetic flux density is 0.1 T, the number of crystals is the least. Further increasing the magnetic flux density produces little change in the crystal quantity. Therefore, the magnetic field inhibits $CaCO_3$ crystallization under specific conditions. The inhibition effect peaks at a magnetic flux density of 0.1 T. Further increasing the magnetic flux density does not enhance the inhibition effect [26,27].

##### *3.1.2.2. Effect of the magnetic field on the form of calcium carbonate crystals in a tunnel drainage pipe*

There are three forms of $CaCO_3$ crystals, namely vaterite, aragonite and calcite. The crystal stability follows an ascending order of vaterite < aragonite < calcite. During crystallization, $CaCO_3$ gradually changes from an unstable form to a stable form. The XRD peaks of $CaCO_3$ crystals were analysed. The diffraction pattern of calcite is typically characterized by multiple narrow peaks. The diffraction pattern of aragonite is characterized by small wide peaks, and the external structure of aragonite is unstable. The diffraction pattern of vaterite typically has a fibre- or coral-like shape. Figs. 4–9 show the XRD scanning of the crystals formed in the PVC pipes of the control and the test groups in the test. When the magnetic flux density is 0.02 T, the high and narrow peaks in the diffraction pattern of the control group show a stable crystal structure, namely calcite. The diffraction pattern of the test groups consists of smaller and wider peaks than those of the control group, indicating that the crystal form becomes unstable under the applied magnetic field.

At a magnetic flux density of 0.05 T, the diffraction peaks of the control group are taller and narrower than those of

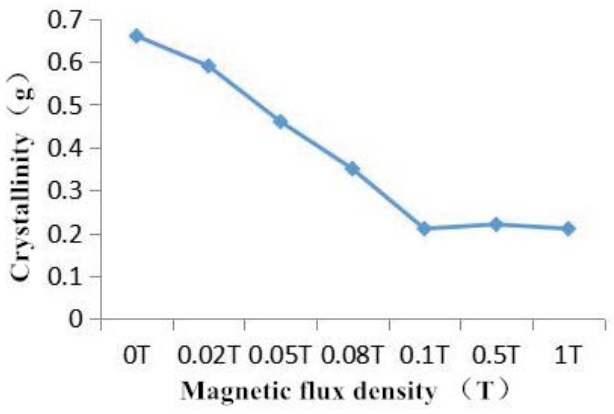


Fig. 3. Average quantity of crystals formed under different magnetic flux densities.

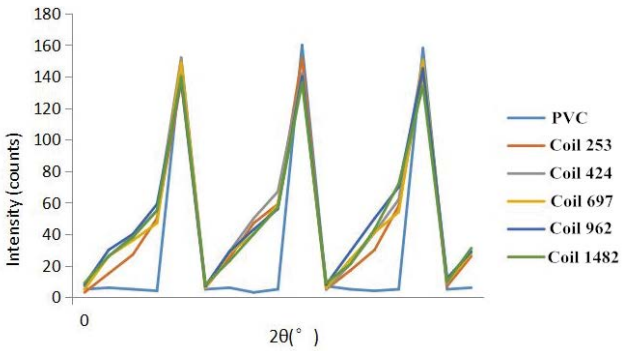


Fig. 4. Diffraction pattern of crystals formed at 0.02 T.

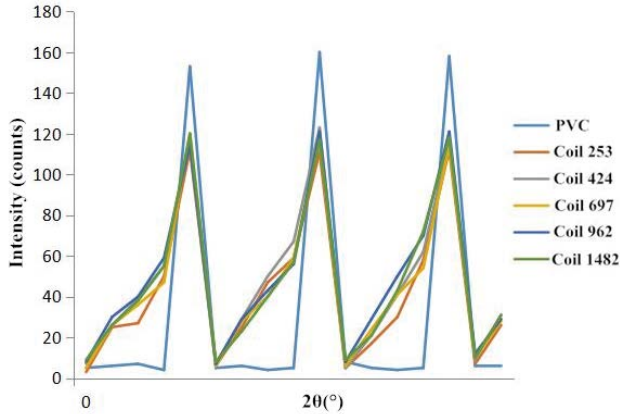


Fig. 5. Diffraction pattern of crystals formed at 0.05 T.

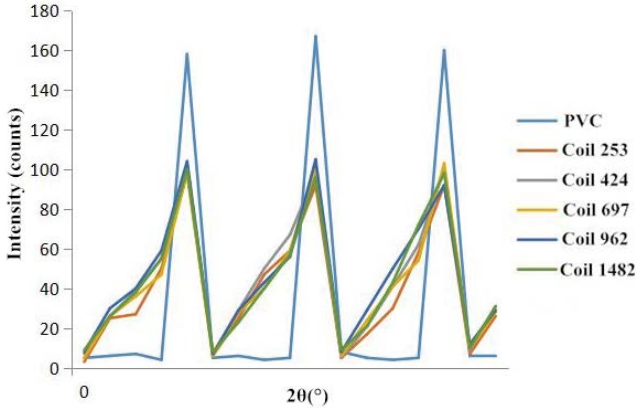


Fig. 6. Diffraction pattern of crystals formed at 0.08 T.

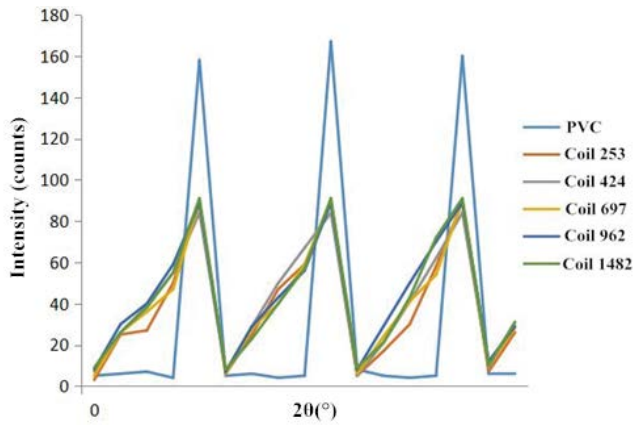


Fig. 7. Diffraction pattern of crystals formed at 0.1 T.

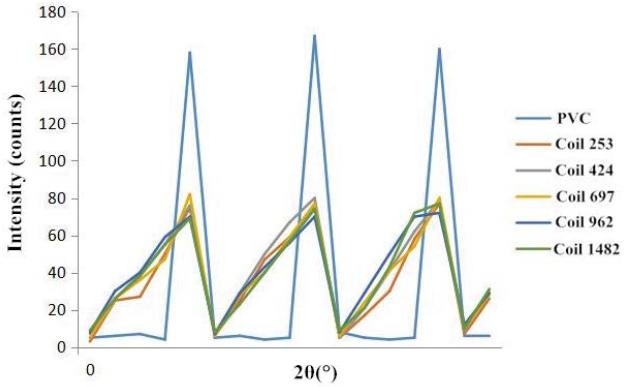


Fig. 8. Diffraction pattern of crystals formed at 0.5 T

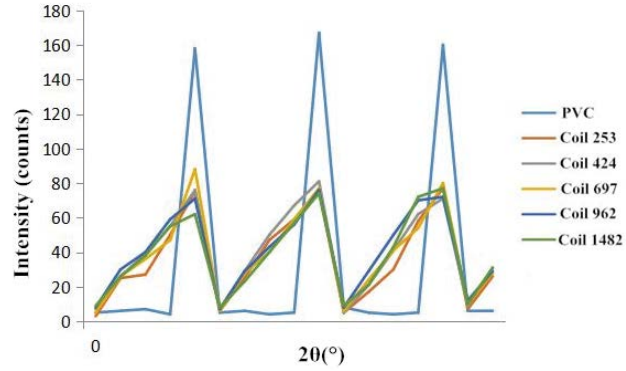


Fig. 9. Diffraction pattern of crystals formed at 1.0 T.

the test groups. In other words, the crystal form of the control group was more stable than those of the test groups. The diffraction peaks of crystals formed at 0.05 T are lower and narrower than those formed at 0.02 T, indicating that the crystal form becomes increasingly unstable as the magnetic flux density increases.

At a magnetic flux density of 0.08 T, the diffraction peaks of the control group are taller and narrower than those of the test groups. This result reveals that the crystal form tends to become unstable under the influence of a magnetic field. The diffraction peaks of crystals formed at 0.05 T are smaller and wider than those of crystals formed at 0.08 T, showing that the crystal form becomes increasingly unstable as the magnetic flux density increases.

At a magnetic flux density of 0.1 T, the diffraction peaks of the control group are taller and narrower than those of the test groups. In other words, the stability of the crystal form has changed under the influence of the magnetic field. The diffraction peaks of crystals formed at 0.08 T are smaller and narrower than those of crystals formed at 0.1 T,

indicating that the crystal form continues to be unstable as the magnetic flux density increases.

At a magnetic flux density of 0.5 T, the diffraction peaks of the control group are taller and narrower than those of the test groups. This result indicates that the control group has a more regular and stable crystal form than the test group and that the crystal form becomes unstable under an applied magnetic field. The diffraction patterns reveal that a more stable crystal form is produced at 0.1 T than at 0.5 T.

For a magnetic flux density of 1.0 T, the tall narrow diffraction peaks of the control group show that the crystal form has become unstable under the applied magnetic field. However, the magnitudes and widths of the diffraction peaks of crystals formed at 1.0 T are not significantly different from those of the crystals formed at 0.5 T. This result indicates that stability of the crystal form does not continue to change beyond a magnetic flux density of 0.5 T.

An analysis of the XRD patterns of crystals formed in the PVC pipes indicates that an applied magnetic field changes the stable crystal form of $CaCO_3$ to an unstable crystal form. However, the crystal form does not change beyond a critical magnetic flux density of 0.5 T.

The test results reveal that a magnetic field inhibits $CaCO_3$ crystallization and destabilizes the crystal form such that the formed crystals can be washed away, thereby reducing the quantity of crystals in the pipe.

### *3.2. Effect of the temperature on crystallization in a tunnel drainage pipe*

#### *3.2.1. Simulation model*

A simulation model was established to investigate the effect of temperature on the inhibition of $CaCO_3$ crystal formation by a magnetic field. The model was a double-layer cubic box (1.872 nm × 1.872 nm × 3.945 nm) composed of 300 water molecules and unit cells of calcite, as shown in Fig. 10.

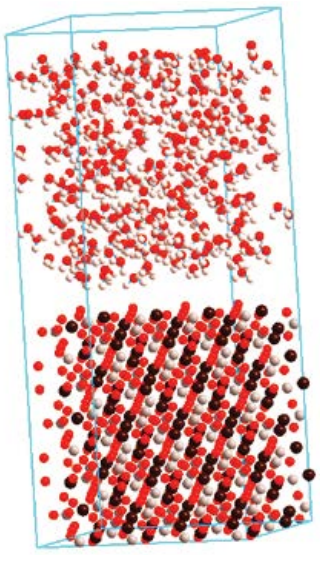

Fig. 10. Model structure.

Most of the $CaCO_3$ found in nature is calcite. Calcite is most stable among the three crystal forms of $CaCO_3$ and it is the main component of the crystals in tunnel drainage pipes in karst areas. Therefore, a calcite model was simulated to be representative of crystal formation in tunnel drainage pipes. The effects of external magnetic field and ambient temperature on the stability of calcite were studied.

The simulation conditions of the model are presented below.

- A consistent-valence forcefield was used to model the water molecules, and both calcium ions and carbanions were modelled as charged Lennard-Jones particles.
- Periodic boundary conditions were applied.
- The canonical NVT ensemble that does not perturb the multidimensional scaling (MDS) trajectory was selected for statistical analysis.
- The leapfrog algorithm was used for numerical integration.
- The simulation time step was set at 1 fs, and the total time of each simulation was set at 160 ps.

#### *3.2.2. Calculation results and analysis*

This model was used to investigate the effect of the magnetic field and temperature on the calcite crystal and the effects of magnetic field and temperature on the stability of calcite crystal were determined. Simulations were performed to track the changing pattern of the peak strength of the radial distribution function of the calcium ions and carbanions that constitute the calcite crystal. A strong peak of the radial distribution function indicates tight bonding between calcium ions and carbanions and a stable $CaCO_3$ crystal structure. In contrast, the weak peak of the radial distribution function indicates loose bonding between calcium ions and carbanions and an unstable $CaCO_3$ crystal structure, showing that the form of calcite crystal has changed. These considerations were used to analyse the influence of the magnetic field and temperature on the $CaCO_3$ crystal form.

The influence of magnetic field on the radial distribution function of calcium ion and carbon anion in unit cells of calcite is discussed by analysing the calculated radial distribution function at 250, 320 and 380 K under a magnetic flux density of 0.01–0.1 T (step size = 0.01 T), 0.1–1 T (step size = 0.1 T) and 1–10 T (step size = 1 T), as shown in Figs. 11–13.

Figs. 11–13 indicate that at the three investigated temperatures, as the magnetic flux density rises, the peak strength of the radial distribution function of the calcium ions and carbanions declines sharply and then undergoes small irregular fluctuations. This result shows that the magnetic field weakens the bond between calcium ions and carbanions that constitute calcite, gradually destabilizing the calcite. Therefore, a magnetic field can change the $CaCO_3$ crystal form under specific conditions to an unstable form. However, at a critical magnetic flux density, the ionic bond between the calcium ions and carbanions becomes sufficiently strong to overcome the Lorentz force generated by the magnetic field. When the two forces become balanced, the magnetic field can no longer significantly change the $CaCO_3$

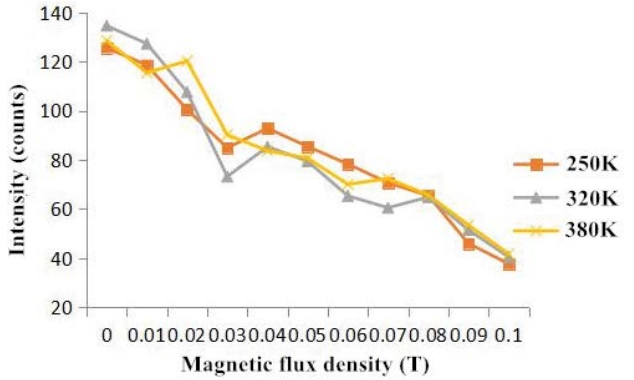


Fig. 11. The relationship between the magnetic flux density and the peak strength at different temperatures (0.01–0.1 T).

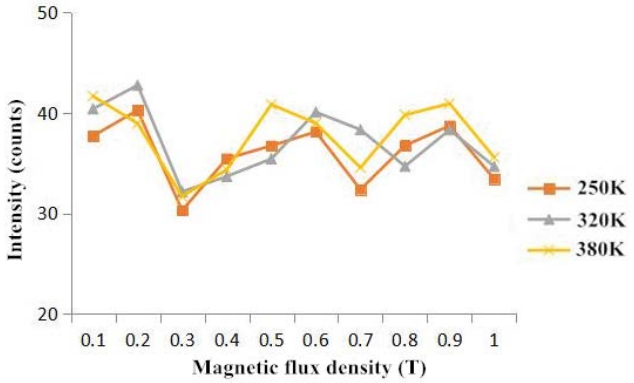


Fig. 12. The relationship between the magnetic flux density and the peak strength at different temperatures (0.1–1 T).

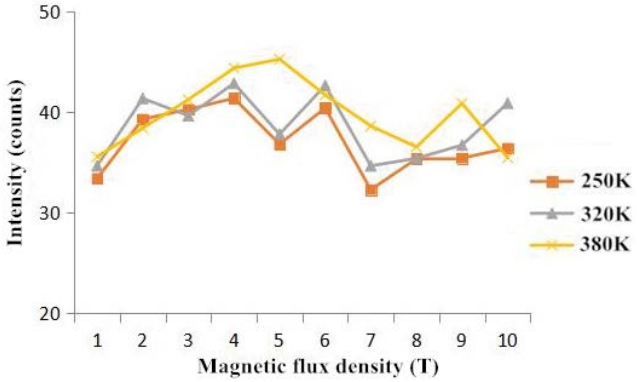


Fig. 13. The relationship between the magnetic flux density and the peak strength at different temperatures (1–10 T).

crystal form. At different temperatures, the peak intensity of radial distribution function of calcium ion and carbon anion is almost the same, indicating that the temperature has little impact on the $CaCO_3$ crystal form.

## 4. Conclusions

Crystallization tests were performed on drainage pipes under six different magnetic field intensities, and simulations were performed on a calcite crystal. The following conclusions were drawn from the results.

- The temperature has little impact on the quantity of crystals formed in drainage pipes under an applied magnetic field.
- Increasing the magnetic flux density destabilizes $CaCO_3$ crystals. However, there is no discernible change in the $CaCO_3$ crystal form when the magnetic flux density exceeds 0.5 T.
- Increasing the magnetic flux density within a certain range decreases the quantity of crystals in a drainage pipe. However, beyond the critical value of 0.1 T, the magnetic flux density cannot effectively inhibit crystallization in the drainage pipes.
- The magnetic field reduces the amount of crystals in drainage pipes by inhibiting the formation of $CaCO_3$ and changing the stable form of $CaCO_3$ crystals to an unstable form that can be washed away.

## Acknowledgements

This research was financially supported by the Scientific Research Project of the Emei Hanyuan Expressway Project (Grant No. LH-HT-45), and the Science and technology project of Guizhou Provincial Department of transportation (Grant No. 2017-123-011).

## References

[1] D. Hasson, M. Avriel, W. Resnick, T. Rozenman, S. Windreich, Calcium carbonate scale deposition on heat transfer surfaces, Desalination, 5 (1968) 107–119.
[2] Z.P. Zhu, Prediction of the $CaCO_3$ minimum solubility in water treatment, Technol. Water Treat., 18 (1992) 343–348.
[3] Z.H. Liu, The dbl model and prediction of calcite dissolution/precipitation rates, Carsologica Sin., 17 (1998) 1–6.
[4] B. Wang, C.J. Li, W. Zhu, Q.L. Xu, Y. Liu, Application of de-fouling technology in pipelines, Corros. Prot. Petrochem. Ind., 25 (2008) 28–30.
[5] A.H. Deng, H.M. Huang, W.J. Ji, Effects of magnetic field on the precipitation of $CaCO_3$, Ind. Water Treat., 10 (2012) 27–30.
[6] W.K. Zhu, X.G. Luo, P. He, et al., Effects of lignin on crystallization of calcium carbonate, Chem. Ind. For. Prod., 6 (2010) 7–12.
[7] M. Luo, Z. Lu, Study of the dynamics of formation of $CaCO_3$ crystal, Fine Chem., 8 (2000) 463–466.
[8] T. Larsen, P. Randhol, M. Lioliou, L.O. Jøsang, T. Østvold, Kinetics of $CaCO_3$ Scale Formation During Core Flooding, Paper presented at the SPE International Oilfield Scale Conference, Paper Number: SPE-114045-MS, Aberdeen, UK, May 2008.
[9] A. Taheri, M. Zahedzadeh, R. Masoudi, F. Alikhani, E. Roayaei, M. Ghanavati, Evaluation of Reservoir Performance Under Water Injection Considering the Effect of Inorganic Scale Deposition in an Iranian Carbonate Oil Reservoir, Paper presented at the 8th European Formation Damage Conference, Paper Number: SPE-121221-MS, Scheveningen, The Netherlands, May 2009.
[10] T.V. Charpentier, A. Neville, S. Baraka-Lokmane, C. Hurtevent, J.-R. Ordonez-Varela, F. Møller Nielsen, V. Eroini, J.H. Olsen, J.A. Ellingsen, Ø. Bache, Evaluation of Anti-fouling Surfaces for Prevention of Mineral Scaling in Sub-surface Safety Valves, Paper presented at the SPE International Oilfield Scale Conference and Exhibition, Paper Number: SPE-169750-MS, Aberdeen, Scotland, May 2014.
[11] D.F. Wang, L.B. Huang, M.M. Wei, T.T. Wang, Y.X. Tian, MD simulation of influence of high voltage static electric field on crystallization of calcium carbonate, Ind. Water Wastewater, 40 (2010) 76–79.

[12] M.K. Story, Surface Temperature Effects on the Fouling Characteristics of Cooling Water, Master Dissertation, Oregon State University, Oregon, The United States, 1974.
[13] H.J. Meyer, The influence of impurities on the growth rate of calcite, J. Cryst. Growth, 66 (1984) 639–646.
[14] Y. Tang, F. Zhang, Z. Cao, W. Jing, Y. Chen, Crystallization of $CaCO_3$ in the presence of sulfate and additives: experimental and molecular dynamics simulation studies, J. Colloid Interface Sci., 377 (2012) 430–437.
[15] M. Bohnet, W. Augustin, Effect of Surface Structure and pH-Value on Fouling Behaviour of Heat Exchangers, International Symposium on Transport Phenomena in Thermal Engineering, 1993, pp. 295–300.
[16] A. Katsifaras, N. Spanos, Effect of inorganic phosphate ions on the spontaneous precipitation of vaterite and on the transformation of vaterite to calcite, J. Cryst. Growth, 204 (1999) 183–190.
[17] Y. Ben Amor, L. Bousselmi, B. Tribollet, E. Triki, Study of the effect of magnesium concentration on the deposit of allotropic forms of calcium carbonate and related carbon steel interface behavior, Electrochim. Acta, 55 (2010) 4820–4826.
[18] C.Y. Tai, M.C. Chang, S.W. Yeh, Synergetic effects of temperature and magnetic field on the aragonite and calcite growth, Chem. Eng. Sci., 66 (2011) 1246–1253.
[19] N. Sánchez-Pastor, A.M. Gigler, J.A. Cruz, S.-H. Park, G. Jordan, L. Fernández-Díaz, Growth of calcium carbonate in the presence of Cr(VI), Cryst. Growth Des., 11 (2011) 3081–3089.
[20] S.J. Jiang, H.G. Yu, C.Y. Liu, Research on the scaling dynamic model of the high salinity system, Appl. Chem. Ind., 40 (2011) 1623–1628.
[21] J. Xu, W. Lan, C. Ren, X.G. Zhou, S. Wang, J. Yuan, Modeling of coupled transfer of water, heat and solute in saline loess considering sodium sulfate crystallization, Cold Reg. Sci. Technol., 189 (2021) 103335, doi: 10.1016/j.coldregions.2021.103335.
[22] H. Lu, P. Tian, L. He, Evaluating the global potential of aquifer thermal energy storage and determining the potential worldwide hotspots driven by socio-economic, geo-hydrologic and climatic conditions, Renewable Sustainable Energy Rev., 112 (2019) 788–796.
[23] L. He, Y. Chen, J. Li, A three-level framework for balancing the tradeoffs among the energy, water, and air-emission implications within the life-cycle shale gas supply chains, Resour. Conserv. Recycl., 133 (2018) 206–228.
[24] X. Li, Z.-Q. Dong, P. Yu, L.-P. Wang, X.-D. Niu, H. Yamaguchi, D.-C. Li, Effect of self-assembly on fluorescence in magnetic multiphase flows and its application on the novel detection for COVID-19, Phys. Fluids, 33 (2021) 042004, doi: 10.1063/5.0048123.
[25] Y.-L. Zou, C. He, H. Cong, Z. Zhang, B. Wang, Analysis of water seepage characteristics and formation mechanisms in seasonal water-rich tunnels in a karst area of Chongqing, Mod. Tunnelling Technol., 51 (2014) 18–27, 45.
[26] C.W. Shi, Z. Wu, F. Yang, Y. Tang, Janus particles with pH switchable properties for high-efficiency adsorption of PPCPs in water, Solid State Sci., 119 (2021) 106702, doi: 10.1016/j.solidstatesciences.2021.106702.
[27] F. Fan, C. Qi, J. Tang, Q. Liu, Thermal and exergy efficiency of magnetohydrodynamic $Fe_3O_4$-$H_2O$ nanofluids flowing through a built-in twisted turbulator corrugated tube under magnetic field, Asia-Pac. J. Chem. Eng. Sci., 15 (2020) e2500, doi: 10.1002/apj.2500.